

1
2
3
4
5
6
7
8
9
10
11
12
13

Supplementary Information

EpiGePT: a Pretrained Transformer model for epigenomics

Zijing Gao^{1,#}, Qiao Liu^{2,#,*}, Wanwen Zeng², Wing Hung Wong^{2,3,*} and Rui Jiang^{1,*}

¹ Ministry of Education Key Laboratory of Bioinformatics, Research Department of Bioinformatics at the Beijing National Research Center for Information Science and Technology, Center for Synthetic and Systems Biology, Department of Automation, Tsinghua University, Beijing 100084, China;

² Department of Statistics, Stanford University, Stanford, CA 94305, USA;

³ Department of Biomedical Data Science, Bio-X Program, Center for Personal Dynamic Regulomes, Stanford University, Stanford, CA 94305, USA;

* To whom correspondence should be addressed.

The first two authors contributed equally.

E-mail: liuqiao@stanford.edu, whwong@stanford.edu, ruijiang@tsinghua.edu.cn

14 Contents

15	Supplementary Texts	3
16	Text S1. Data splitting strategy for model training.....	3
17	Text S2. System design and implementation of the web server.....	4
18	Text S3. Running time of the EpiGePT and baseline methods.	5
19	Text S4. Implementation of Enformer model and Enformer+	6
20	Supplementary Figures.....	7
21	Fig. S1.....	7
22	Fig. S2.....	8
23	Fig. S3.....	10
24	Fig. S4.....	12
25	Fig. S5.....	14
26	Fig. S6.....	15
27	Fig. S7.....	17
28	Fig. S8.....	18
29	Supplementary Tables	19
30	References	20

31 **Supplementary Texts**

32 **Text S1. Data splitting strategy for model training.**

33 To comprehensively validate the performance of EpiGePT in predicting chromatin accessibility,
34 we adopted three different data splitting strategies in the DNase¹ prediction experiment to
35 verify the model's prediction ability when facing new genomic regions and cell types, which
36 can meet researchers' usage needs to the maximum extent. Firstly, cross-cell type prediction
37 refers to splitting the training and testing sets according to cell types in the same genomic
38 region, where the cell types in the testing set have not appeared in the training set (Figs. S1B).
39 Secondly, cross-genomic region prediction refers to splitting the training and testing sets
40 according to genomic regions in the same cell type (Figs. S1A). Thirdly, simultaneous cross-
41 cell type and genomic region prediction, where the prediction can be performed in completely
42 novel cell types and genomic regions with the expression of transcription factors in that cell
43 type. The training set needs to subset both cell types and genomic regions (Figs. S1C). To
44 complete the latter two auxiliary predictions, we also split the data into 5 folds according to
45 both cell types and genomic regions, so that both cross-validation can be performed in one
46 round of training, but this will also reduce the amount of training and testing data.

47 **Text S2. System design and implementation of the web server.**

48 EpiGePT-online runs on a Linux-based Apache web server (<https://www.apache.org>) and
49 utilizes the Bootstrap v3.3.7 framework (<https://getbootstrap.com/docs/3.3/>) for its web-
50 frontend display. The backend of the server uses PHP v7.4.5 (<http://www.php.net>). The
51 platform is compatible with the majority of mainstream web browsers, including Google
52 Chrome, Firefox, Microsoft Edge, and Apple Safari.

53 **Text S3. Running time of the EpiGePT and baseline methods.**

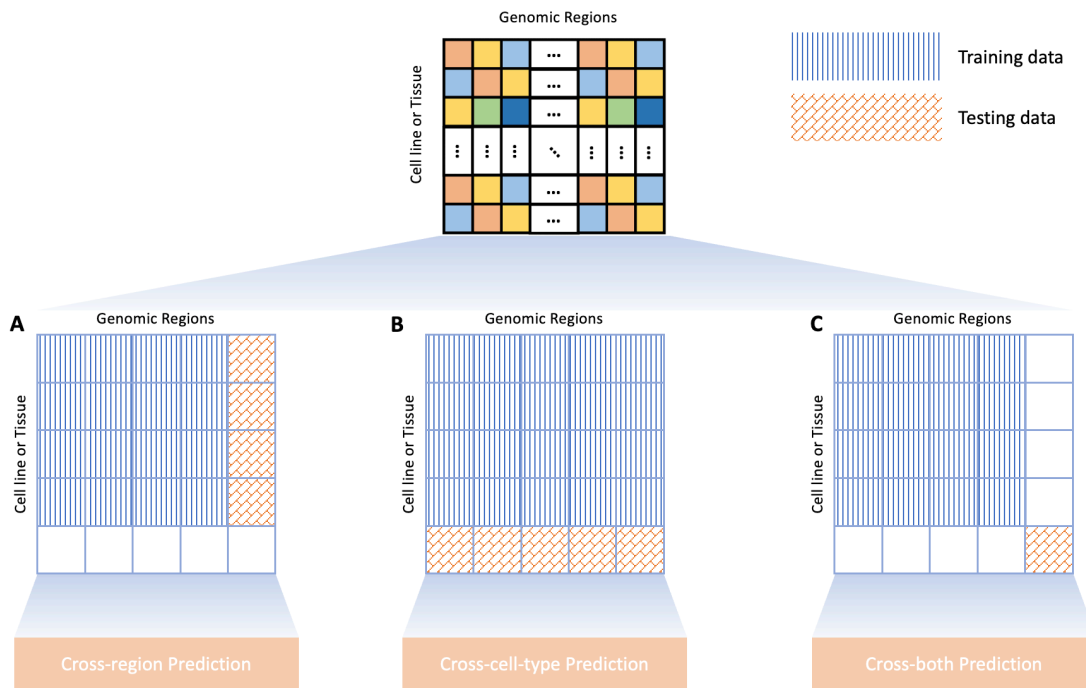
54 To demonstrate the computational efficiency of our model, we recorded the runtime of
55 EpiGePT and baseline methods for one epoch on two sets of experiments, with different data
56 sizes and input sequence lengths. Firstly, in the DNase signal prediction experiment on 129
57 cell types, with an input sequence length of 10kbp and using the same training data, Enformer
58 requires approximately 3 hours and 4 minutes to complete one epoch, while EpiGePT only
59 takes 2 hours and 17 minutes. In contrast, ChromDragoNN², which uses a genomic bin rather
60 than a long region as the model input, requires 24 hours for pre-training and 8 hours for fine-
61 tuning. In this case, the batch size of ChromDragoNN was set to 1024, which is equivalent to
62 EpiGePT using a batch size of around 20. This modeling and computation approach presents
63 challenges in terms of computational efficiency when dealing with large amounts of data.
64 DeepCAGE³ faces similar efficiency issues using the same approach. Even with a batch size
65 of 256 on a single GPU, it still takes nearly 10 hours to complete one epoch of training.
66 Secondly, we also recorded the running time of the models under larger-scale data and longer
67 input sequences. When the number of input genomic bins increased from 50 to 1000, which
68 corresponds to an input sequence length of approximately 128k, EpiGePT took approximately
69 3 hours to complete one epoch of training on 20 cell lines and 13,300 genomic regions, while
70 Enformer required approximately 27 hours to train one epoch, as it required a longer input
71 sequence of approximately 190kbp. Furthermore, EpiGePT without TF module (EpiGePT-seq)
72 had approximately 1/4 of the parameters of Enformer and took approximately 2 hours and 40
73 minutes to train. In terms of performance, EpiGePT-seq performed similarly to Enformer on
74 this dataset. This also explains why we chose to simplify the pure sequence model rather than
75 directly adding a TF module to Enformer.

76 **Text S4. Implementation of Enformer model and Enformer+.**

77 To ensure a fair comparison between models and prevent the possibility of information
78 leakage, we implemented the Enformer⁴ model ourselves and trained it on our own collected
79 data. Due to differences in dataset size and partitioning compared to Enformer, we reduced
80 the number of encoder layers in Enformer to prevent overfitting. Thus, we reduced the number
81 of encoder layers in Enformer to 3. Additionally, we introduced Enformer+ to enable a fair
82 comparison between EpiGePT and Enformer in locus-level prediction. As Enformer takes only
83 the DNA sequence as input, it tends to predict the same values for the same locus in different
84 cell types, resulting in a loss of locus-level prediction ability. To address this, we incorporated
85 the binding status and expression of the same transcription factors in Enformer+, and
86 compared it to EpiGePT's performance on the same tasks.

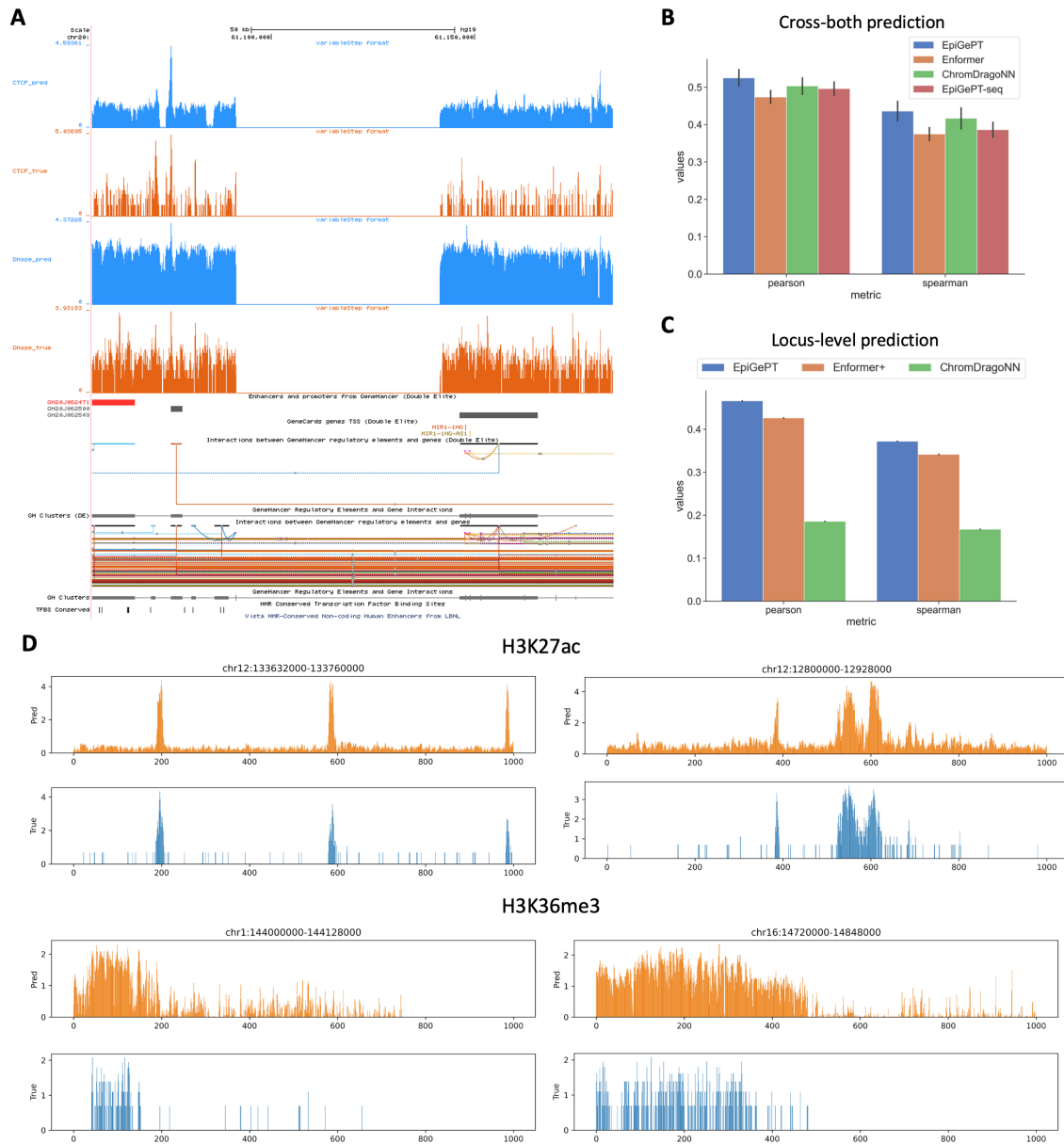
87 **Supplementary Figures**

88 **Fig. S1**



89 **Fig. S1. Three data partitioning strategies for model training and testing.** (A) Cross
90 genomic region prediction. The training and testing datasets utilized the expression profiles of
91 identical cell types, but were evaluated on novel genomic regions for prediction. (B) Cross cell
92 type prediction. The training and testing datasets utilized the same genomic regions, but were
93 evaluated on novel cell types for prediction. (C) Cross genomic region and cell type prediction.
94 The cell types and genomic regions used in the training and test sets were both different.

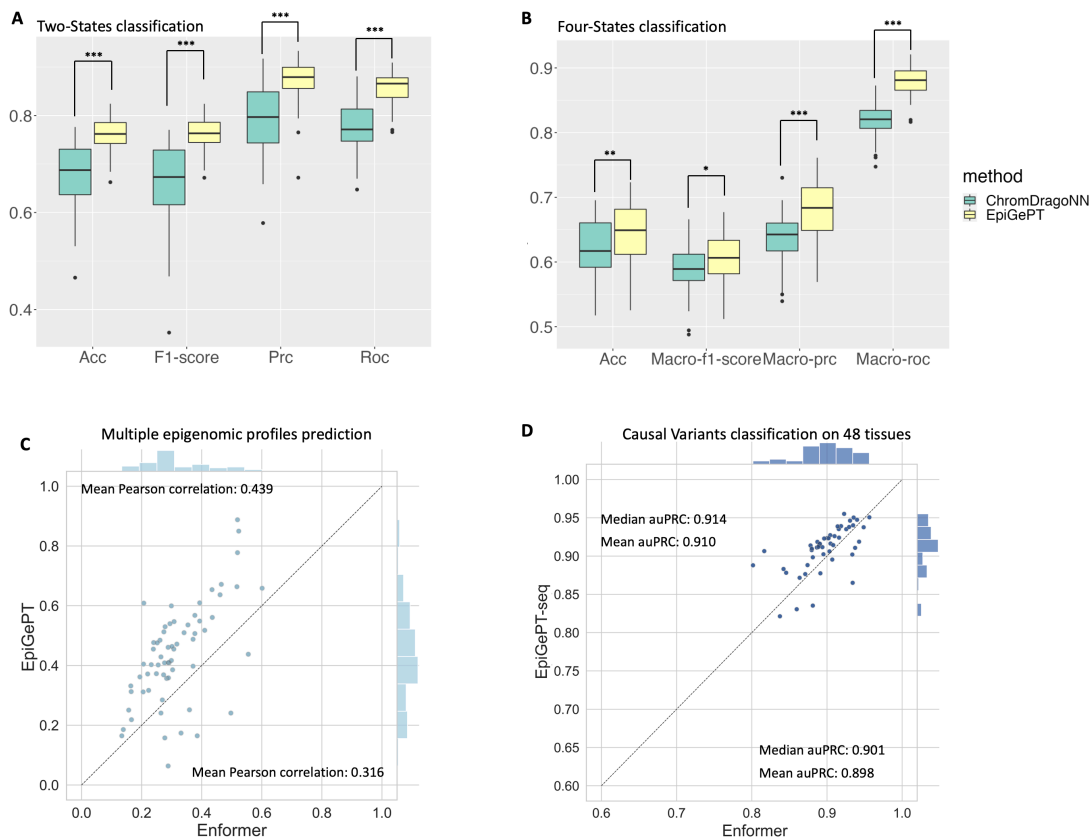
95 **Fig. S2**



96 **Fig. S2. EpiGePT's performance in predicting DNase-seq and other epigenetic signals**
 97 **is demonstrated in (A) through visualization of predicted results for DNase and CTCF signals.**
 98 EpiGePT is able to make accurate predictions for these signals, as well as for the regulatory
 99 relationships within a genomic region of 20th chromosome ranging from 61,100,000 to
 100 61,150,000. (B) EpiGePT and baseline methods were compared for their performance in
 101 predicting epigenetic signals in new cell types and genomic regions (cross-both prediction).
 102 The left panel shows the Pearson correlation coefficient, and the right panel shows the

103 Spearman correlation coefficient. (C) Locus level prediction of DNase signal. We predicted a
104 value for each genomic locus, and calculated the correlation coefficient between the predicted
105 values and true values for the same locus in different cell types. (D) Visualization of predicted
106 signals, such as the comparison between predicted and true values in a 128kbp region (from
107 133,632,000 to 133,760,000) on chromosome 12, shows that the presence of a large number
108 of zeros in both the true and predicted signals can limit the correlation between the two signals.

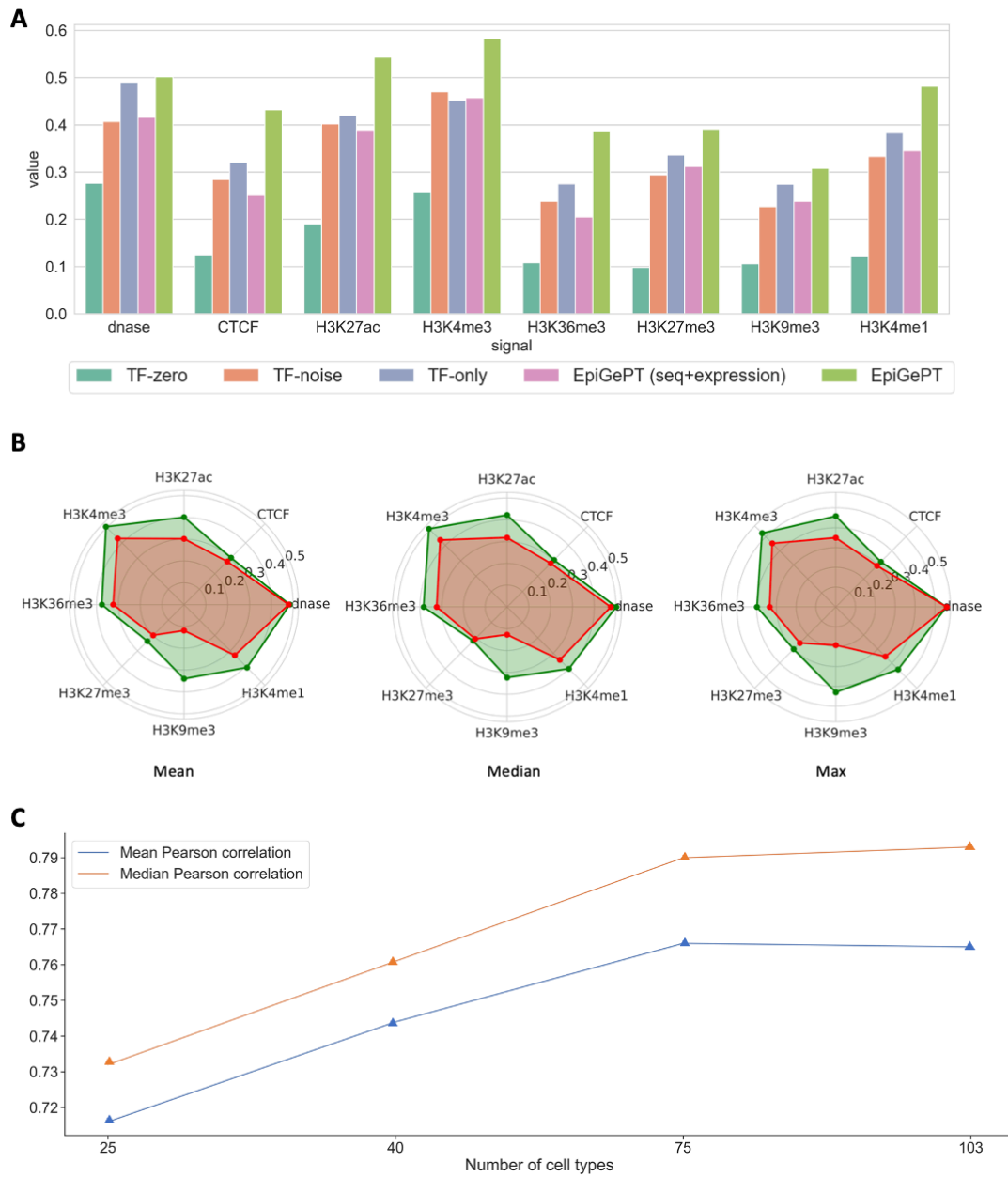
109 **Fig. S3**



110 **Fig. S3. Performance of EpiGePT and baseline methods on chromatin states**
 111 **classification, multiple epigenomic profiles prediction and causal variants**
 112 **classification.** (A) Binary classification of chromatin states for distinguishing functional
 113 regions on the chromatin based on the annotation data from ChromHMM-15-states. (B) Four-
 114 class chromatin state classification is used to distinguish functional regions on the chromatin,
 115 including TSS, potential enhancers, other functional regions, and non-functional regions
 116 based on the annotation data from ChromHMM-15-states. * indicates that the p -value is less
 117 than 0.005 under a one-sided Wilcoxon hypothesis test, ** indicates that the p -value is less
 118 than 0.005 under a one-sided Wilcoxon hypothesis test, and *** indicates that the p -value is
 119 less than $1e-3$ under this hypothesis test. (C) Cross-cell-type prediction of 8 epigenomic
 120 signals at 8 test cell types. Each dot denotes the Pearson correlation coefficient of the predicted
 121 signals and true signals at the specific cell types on a specific epigenomic signal. (D) The performance

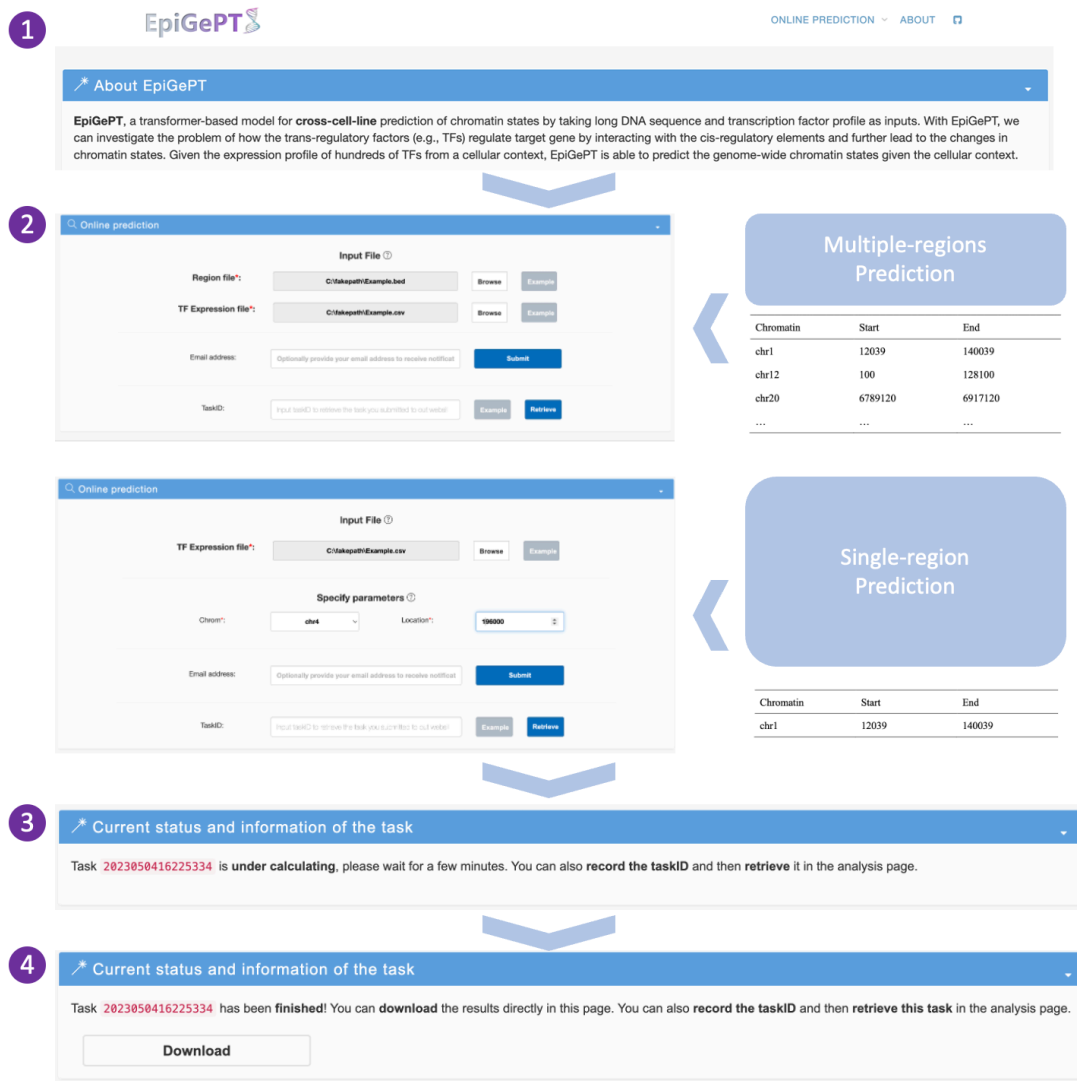
122 of EpiGePT and Enformer in discriminating causal eQTLs across 48 tissues, each dot
123 representing the average auPRC obtained from 5-fold cross-validation on a specific tissue.

124 **Fig. S4**

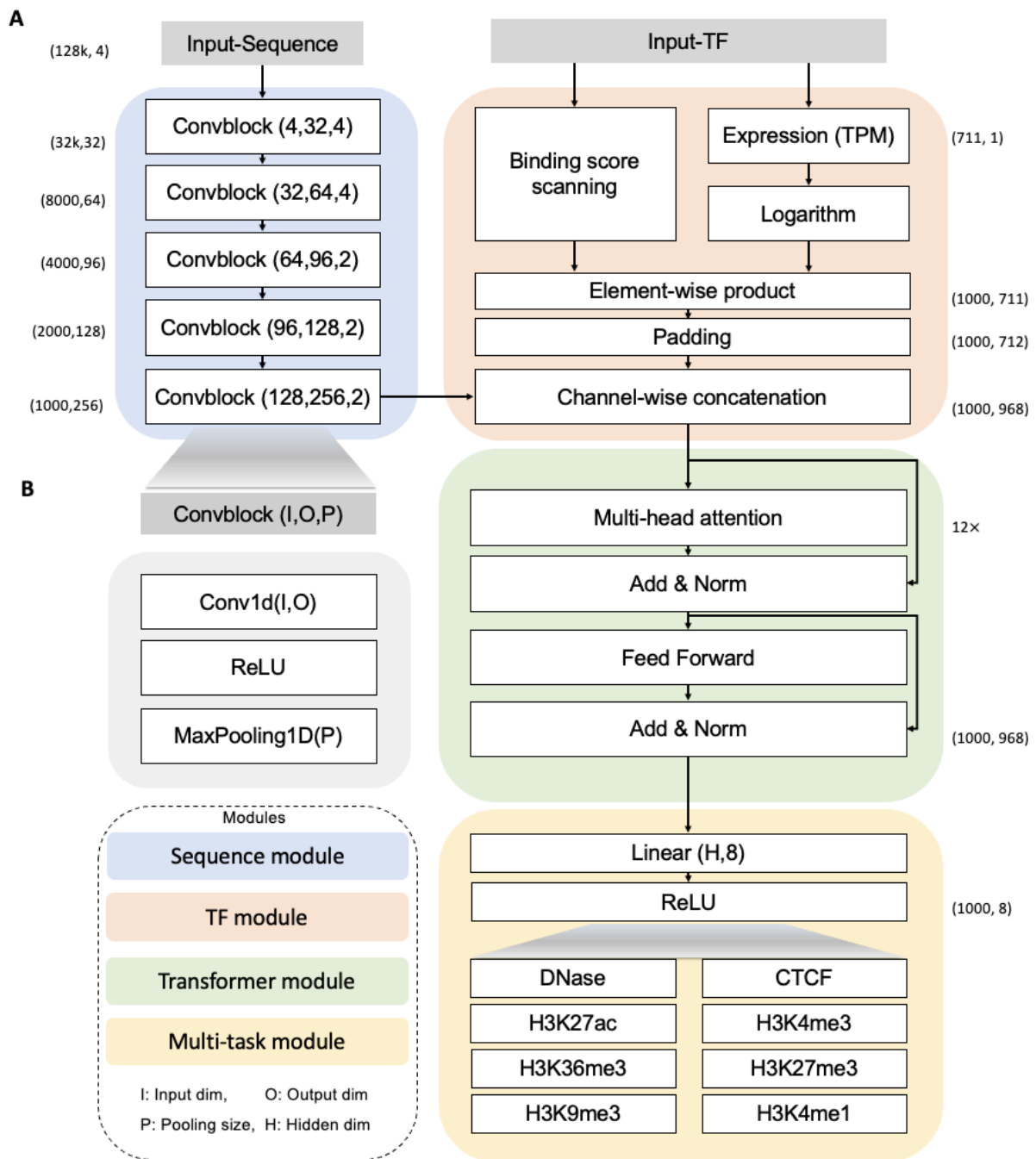


125 **Fig. S4. Ablation analysis of the EpiGePT model.** (A) Ablation analysis on the TF module
 126 and the Sequence module, we observed a decrease in predictive performance for each
 127 module across eight chromatin epigenetic signals, as evidenced by a reduction in Pearson
 128 correlation coefficient. (B) Ablation analysis on the Multi-task module. The green shaded area
 129 in the figure represents the results of multi-signal cross-cell-type predictions, while the red
 130 shaded area represents the results of training and predicting on each signal individually. It can

131 be observed that the multi-task module has a positive effect on the model performance across
132 all signals. (C) Ablation analysis of the number of the training cell types. When the number of
133 training cell types increases while the number of testing cell types remains constant, there is
134 an increasing trend in performance as the number of training cell types increases.

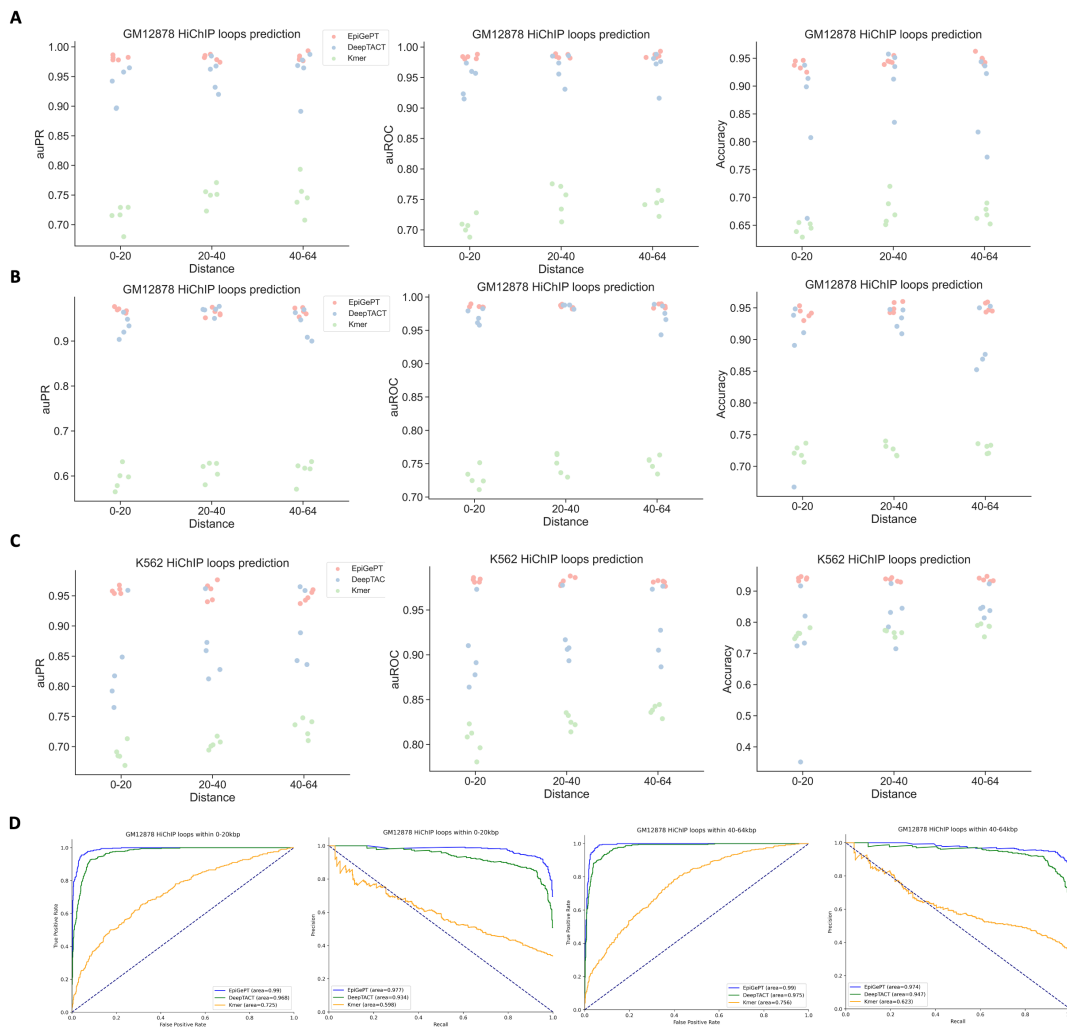


136 **Fig. S5. Case application of the EpiGePT-online.** Users can choose either single locus
 137 annotation or multi-region annotation on EpiGePT-online, and each genomic region requires
 138 a length of 128kbp. Users need to upload the TPM values of transcription factors expression
 139 simultaneously. After annotation, users can enter the result page and download the predicted
 140 files. The prediction accuracy is 128bp genomic bin, and users can obtain the predicted signals
 141 of these eight epigenetic modifications.



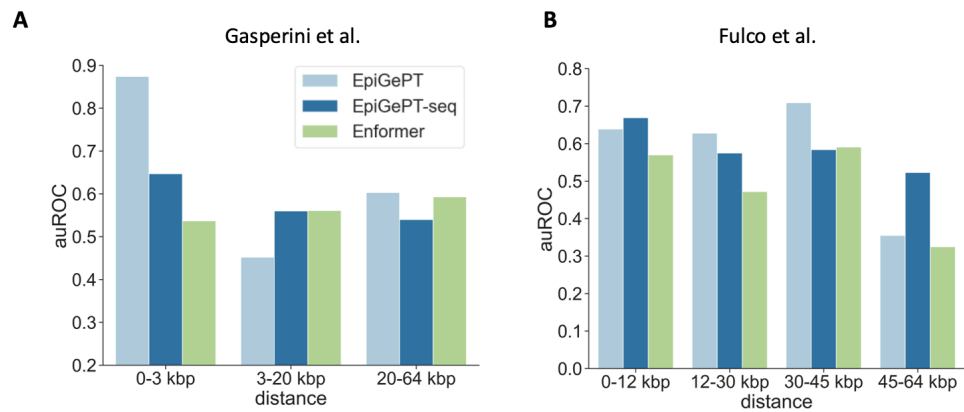
143 **Fig S6. Model architecture of EpiGePT for multiple epigenomic signals prediction.** (A)
 144 The computational process of EpiGePT. The sequence module employs a stack of five
 145 convolutional layers followed by pooling operations, resulting in representations that capture
 146 sequence patterns. The TF module integrates motif binding information and gene expression
 147 data to represent cell-specific information. The Transformer module takes the genomic bin

148 sequences mentioned above as input and learns the interaction relationships between bins,
149 capturing the interactions among them. Finally, the obtained embeddings are mapped to the
150 eight types of epigenomic signals through a fully connected layer. (B) Specific details of the
151 convolutional block involve the fusion of 1D convolution, ReLU activation function, and max
152 pooling operation to achieve changes in the feature dimension O and extract bin-level features.
153



155 **Fig. S7. The fine-tuning performance of the EpiGePT model on predicting potential**
 156 **enhancer-promoter regulatory networks.** (A) The performance (measured by auROC and
 157 auPRC) of the fine-tuned EpiGePT model and baseline methods (DeepTACT and Kmer) on
 158 HiChIP loops data in distinguishing enhancer-gene pairs at various distance ranges (0-20 kbp,
 159 20-40 kbp and 40-64 kbp). (B) The performance of the fine-tuned EpiGePT model and
 160 baseline methods on HiChIP loops data in distinguishing enhancer-gene pairs under 1:2
 161 positive-negative sample ratio on GM12878 cell line. (C) The performance of the fine-tuned
 162 EpiGePT model and baseline methods on HiChIP loops data in distinguishing enhancer-gene
 163 pairs under 1:2 positive-negative sample ratio on K562 cell line. (D) The ROC and PR curves
 164 of EpiGePT and baseline methods for predicting HiChIP loops from the GM12878 cell type.

165 **Fig. S8**



166 **Fig. S8. The performance (auROC) of attention score of EpiGePT in distinguishing**
167 **regulatory element-gene pairs at different distance ranges.** (A) The performance of
168 EpiGePT in distinguishing enhancer-gene pairs at different distance ranges on the data from
169 Gasperini et al⁵. (B) The performance of EpiGePT in distinguishing enhancer-gene pairs at
170 different distance ranges on the data from Fulco et al⁶.

Supplementary Tables

Table S1. The information of DNase-seq bam file across 129 biosamples from the ENCODE⁷ project.

Table S2. The information of RNA-seq tab-separated values (tsv) file across 129 biosamples from the ENCODE project.

Table S3. The information of DNase-seq, CTCF and other six Histone markers bam file across 28 cell lines or tissues from the ENCODE project.

Table S4. The information of RNA-seq tab-separated values (tsv) file across 28 cell lines or tissues from the ENCODE project.

Table S5. The preprocessed expression data of 711 human transcription factors from the ENCODE project across 129 biosamples.

Table S6. The preprocessed expression data of 711 human transcription factors from the ENCODE project across 28 cell lines or tissues.

Table S7. The order and names of epigenomes of the expression matrices across 56 epigenomes from the ROADMAP⁸ project.

Table S8. The preprocessed expression data of 642 human transcription factors across 56 epigenomes from the ROADMAP project.

References

1. Song, L. & Crawford, G.E. DNase-seq: a high-resolution technique for mapping active gene regulatory elements across the genome from mammalian cells. *Cold Spring Harbor Protocols* **2010**, pdb. prot5384 (2010).
2. Nair, S., Kim, D.S., Perricone, J. & Kundaje, A. Integrating regulatory DNA sequence and gene expression to predict genome-wide chromatin accessibility across cellular contexts. *Bioinformatics* **35**, i108-i116 (2019).
3. Liu, Q., Hua, K., Zhang, X., Wong, W.H. & Jiang, R. DeepCAGE: incorporating transcription factors in genome-wide prediction of chromatin accessibility. *Genomics, Proteomics & Bioinformatics* **20**, 496-507 (2022).
4. Avsec, Ž. et al. Effective gene expression prediction from sequence by integrating long-range interactions. *Nature methods* **18**, 1196-1203 (2021).
5. Gasperini, M. et al. A genome-wide framework for mapping gene regulation via cellular genetic screens. *Cell* **176**, 377-390. e319 (2019).
6. Fulco, C.P. et al. Activity-by-contact model of enhancer–promoter regulation from thousands of CRISPR perturbations. *Nature genetics* **51**, 1664-1669 (2019).
7. Consortium, E.P. An integrated encyclopedia of DNA elements in the human genome. *Nature* **489**, 57 (2012).
8. Bernstein, B.E. et al. The NIH roadmap epigenomics mapping consortium. *Nature biotechnology* **28**, 1045-1048 (2010).